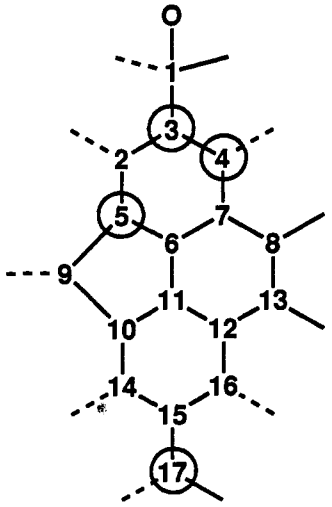

Figure 1. Seventeen types of cluster carbons in $C_{60}(OsO_4)$(4-*tert*-butylpyridine)$_2$.[8] Dashed lines indicate bonds between symmetry-related carbons. Circles indicate carbon types with integratable satellites.

Table I. Experimental and Calculated Ratios of Satellite Integration to Central Peak Integration in ^{13}C-Enriched $C_{60}(OsO_4)$(4-*tert*-butylpyridine)$_2$

carbon type	experimental ratio	statistical ratio
3	0.22	0.24
4	0.18	0.16
5	0.22	0.24
17	0.14	0.16

vaporization apparatus.[3] Mass spectral analysis of the C_{60} indicated 5.0 mol % ^{13}C. This material was converted to $C_{60}(OsO_4)$(4-*tert*-butylpyridine)$_2$[7] and analyzed by ^{13}C NMR. Carbon types 3, 4, 5, and 17 in $C_{60}(OsO_4)$(4-*tert*-butylpyridine)$_2$ are well separated from the other peaks,[8] and the ^{13}C satellites could be integrated relative to the central peaks (Figure 1, Table I).[9] The observed satellite peaks are composed of doublets, quartets, and one-half of the triplet pattern, while the central peak corresponds to singlets plus one-half of the triplet pattern.

If the ^{13}C's are randomly distributed in C_{60}, the ratio of the satellite integration to the central peak integration is described by eq 1, where s_n, d_n, t_n, and q_n correspond to the singlet, doublet, triplet, and quartet signals per $^{13}C_n{}^{12}C_{(60-n)}$ molecule, and I_n corresponds to the intensity of the m/z 720 + n peak in the mass spectrum. Carbon types 3 and 5 each couple with three adjacent nonequivalent carbons, and carbon types 4 and 17 each couple with two adjacent nonequivalent carbons. Assuming random ^{13}C distributions, s_n, d_n, t_n, and q_n are given by eqs 2–5 for carbon types 3 and 5 and by eqs 6–9 for carbon types 4 and 17 (x = 2 for type 17, and x = 4 for type 4). The satellite to central peak ratios calculated for random ^{13}C distribution within the carbon clusters using eqs 1–9 and the mass spectrum[10] agree very well with the experimental values (Table I). In contrast, if the ^{13}C's were incorporated into C_{60} as intact C_m units with $m \geq 2$, these ratios would be much larger, approximately 4 for carbon types 3 and 5, and approximately 1.5 for carbon types 4 and 17.

$$\frac{\text{satellite integration}}{\text{central peak integration}} = \frac{\sum_n \left(d_n + \frac{t_n}{2} + q_n\right) I_n}{\sum_n \left(s_n + \frac{t_n}{2}\right) I_n} \quad (1)$$

$$s_n(3,5) = \frac{4n}{60} - d_n(3,5) - t_n(3,5) - q_n(3,5) \quad (2)$$

$$d_n(3,5) = \frac{12n}{60}\left(\frac{n-1}{59}\right)\left(1 - \frac{n-2}{58}\right)\left(1 - \frac{n-2}{57}\right) \quad (3)$$

$$t_n(3,5) = \frac{12n}{60}\left(\frac{n-1}{59}\right)\left(\frac{n-2}{58}\right)\left(1 - \frac{n-3}{57}\right) \quad (4)$$

$$q_n(3,5) = \frac{4n}{60}\left(\frac{n-1}{59}\right)\left(\frac{n-2}{58}\right)\left(\frac{n-3}{57}\right) \quad (5)$$

$$s_n(4,17) = \frac{xn}{60} - d_n(4,17) - t_n(4,17) \quad (6)$$

$$d_n(4,17) = \frac{2xn}{60}\left(\frac{n-1}{59}\right)\left(1 - \frac{n-2}{58}\right) \quad (7)$$

$$t_n(4,17) = \frac{xn}{60}\left(\frac{n-1}{59}\right)\left(\frac{n-2}{58}\right) \quad (8)$$

$$q_n(4,17) = 0 \quad (9)$$

From the examination of mass spectral data, Heath concluded, "The chemical species initially ejected from the graphite rods in the carbon arc are...atoms and possibly dimers."[3] From this study, we conclude that if the initially ejected species are dimers, the carbon atoms of the C_2 units must scramble either before or after condensation into the C_{60} cluster, as they do not remain connected in the isolated C_{60}.

Acknowledgment. J.M.H. is grateful to the National Science Foundation (Presidential Young Investigator Award, CHE-8857453), the Camille and Henry Dreyfus Foundation (New Faculty Grant), the Merck Sharp & Dohme Research Laboratories (postdoctoral fellowship for A.M.), the Shell Oil Company Foundation (Shell Faculty Fellowship), Xerox Corporation, Monsanto Company, and Hoffman-La Roche for financial support. S.L. thanks Syntex Corporation for a graduate fellowship.

Registry No. 1, 134962-77-9; ^{13}C, 14762-74-4.

(9) Since there is no NOE and the acquisition parameters were optimized for the approximately 4 s T_1 of carbon types 2–17, the integration is quite reliable. The ratios of the integrals of carbon types 3, 4, 5, and 17 (including the ^{13}C satellites) are within 3% of the expected ratios, i.e., 4:4:4:2.

(10) MS: m/z (intensity) 720 (21 693), 721 (24 094), 722 (20 970), 723 (17 726), 724 (13 672), 725 (10 780), 726 (7205), 727 (5285), 728 (3362), 729 (2137), 730 (1341), 731 (813), 732 (495), 733 (246), 734 (311), 735 (155).

Potential-Dependent Surface Raman Spectroscopy of Buckminsterfullerene Films on Gold: Vibrational Characteristics of Anionic versus Neutral C_{60}

Yun Zhang, Gregory Edens, and Michael J. Weaver*

Department of Chemistry, Purdue University
West Lafayette, Indiana 47907

Received September 3, 1991

We report here real-time surface-enhanced Raman (SER) spectra for films of buckminsterfullerene (C_{60}) on gold in acetonitrile observed during cyclic voltammetric potential excursions. The results provide the first vibrational spectra for the C_{60} monoanion; they indicate that reduction induces significant perturbations in the bonding and symmetry characteristics of C_{60}.

Several Raman and infrared studies have been reported for neutral C_{60}.[1-3] Most findings are in harmony with the predicted

(1) (a) Bethune, D. S.; Meijer, G.; Tang, W. C.; Rosen, H. J. *Chem. Phys. Lett.* **1990**, *174*, 219. (b) Bethune, D. S.; Meijer, G.; Tang, W. C.; Rosen, H. J.; Golden, W. G.; Seki, H.; Brown, C. A.; de Vries, M. S. *Chem. Phys. Lett.* **1991**, *179*, 181.

(2) Garrell, R. L.; Herne, T. M.; Szafranski, C. A.; Diederich, F.; Ettl, F.; Whetten, R. L. *J. Am. Chem. Soc.* **1991**, *113*, 6302.

(3) (a) Krätschmer, W.; Fostiropoulos, K.; Huffman, D. R. *Chem. Phys. Lett.* **1990**, *170*, 167. (b) Cox, D. M.; Behal, S.; Disko, M.; Gorun, S. M.; Greaney, M.; Hsu, C. S.; Kollin, E. B.; Millar, J.; Robbins, J.; Robbins, W.; Sherwood, R. D.; Tindall, P. *J. Am. Chem. Soc.* **1991**, *113*, 2940. (c) Huang, Y.; Gilson, D. F. R.; Butler, I. S. *J. Phys. Chem.* **1991**, *95*, 5723.

0002-7863/91/1513-9395$02.50/0

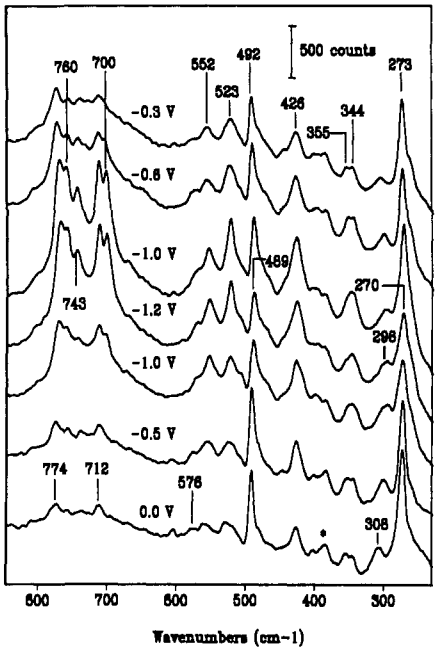

Figure 1. Potential-dependent SER spectral sequence in 240–840-cm^{-1} region, obtained during 10 mV s^{-1} voltammogram from 0 to −1.2 V and return (vs Fc^+/Fc) for ca. five monolayer C_{60} film on gold in acetonitrile containing 0.1 M TBAP. Each spectrum was acquired in 8 s. The peak designated by the asterisk is due to acetonitrile. Raman excitation was at 647.1 nm, with 20-mW power; bandpass was 6 cm^{-1}.

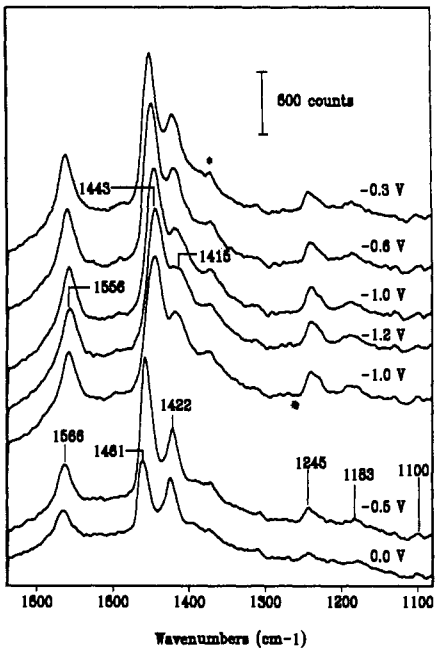

Figure 2. As in Figure 1, but for 1080–1620-cm^{-1} region.

Table I. Summary of SERS Band Frequencies (cm^{-1}) for C_{60} and C_{60}^- and Comparison with Raman Spectra for Bulk-Phase C_{60}

C_{60}^{-} [a,e]	C_{60} [b,e]	C_{60} [c,e]	assignment [d]
270 (s)	273 (s)	273 (s)	H_g squashing
420 (s)	426 (m)	437 (m)	H_g
489 (s)	492 (s)	496 (s)	A_g breathing
520 (s)	523 (w)	[527]	F_{1u}
576 (w)	576 (w)	[577]	F_{1u}
712 (s), 700 (s)	712 (w)	710 (w)	H_g
743 (m)	743 (w)		?
770 (s), 760 (s)	774 (m)	774 (m)	H_g
1100 (w)	1100 (w)	1099 (w)	H_g
1183 (w)	1183 (vw)	[1183]	F_{1u}
1245 (m)	1245 (w)	1250 (w)	H_g
1415 (w)	1422 (m)	1428 (m), [1428]	H_g, F_{1u}
1443 (s)	1461 (s)	1470 (vs)	A_g "pentagonal pinch"
1556 (m)	1566 (m)	1575 (m)	H_g

[a] Major SERS band frequencies for C_{60}^-, measured for C_{60} film on gold in acetonitrile at potentials between −1.0 and −1.2 V vs $Fc^{+/0}$. [b] Major SERS frequencies for C_{60}, obtained as in footnote *a* at potentials positive of ca. −0.6 V vs $Fc^{+/0}$. [c] Corresponding bulk-phase Raman band frequencies for solid C_{60}, taken from ref 1b. Values given in brackets refer to IR-active bands. [d] Vibrational band assignments, from ref 1b. [e] Band intensities: vw = very weak, w = weak, m = medium, s = strong, vs = very strong.

expectation of only 10 Raman active and four infrared-active vibrations.[4,5] Especially given this high degree of symmetry, it is of interest to examine the effects of adding an electron (or electrons); a reduction in symmetry might be anticipated due to Jahn–Teller distortions, along with possible changes in the skeletal force constants and hence vibrational frequencies. Reversible electroreduction of solution-phase C_{60} in up to four one-electron steps occurs in suitable nonaqueous media.[3b,5,6] The UV–visible spectroelectrochemistry of these states exhibits significant redox-induced spectral shifts.[6] The reversible electroreduction in acetonitrile of C_{60} films formed by solution evaporation on Pt, Au, or glassy carbon surfaces has recently been demonstrated.[7] Given that extended (i.e., multilayer) films as well as adsorbates on suitably roughened gold electrodes exhibit stable as well as intense SER spectra (SERS),[8] this observation suggests that SERS could provide a powerful means of examining the sensitivity of the C_{60} vibrational properties to the cluster oxidation state.

The gold electrode, 4 mm in diameter sheathed in Teflon, was rendered SERS-active by means of the oxidation–reduction procedure described in ref 9, and was rinsed with acetonitrile prior to use. The C_{60} films were prepared by evaporating on the surface a few microliters of a ca. 0.01–0.1 mM solution in dichloromethane.[7] The solid C_{60} sample was prepared and purified according to procedures in ref 5. Acetonitrile was distilled over CaH_2, and tetrabutylammonium perchlorate (TBAP) was recrystallized twice from water. An equimolar mixture of ferrocenium/ferrocene ($Fc^{+/0}$) in acetonitrile (contained in a separate compartment) was used as the reference electrode. Cyclic voltammograms run from 0 V to up to −2 V (versus $Fc^{+/0}$) for the C_{60} films in acetonitrile containing 0.1 M TBAP are similar to those reported in ref 7. (The charge contained under the voltammetric waves provides an additional assay of the film thickness.) Sequences of SER spectra were recorded during such cyclic voltammograms by means of a SPEX Model 1877 spectrometer equipped with a Photometrics PM 512 CCD detector (see ref 10 for other details). Laser excitation was a Kr^+ laser operated at 647 nm with ca. 20 mW power on the sample. Individual spectra could be obtained every few seconds during the potential excursion, allowing the voltammetric features to be matched with the observed spectral changes.[11]

(4) (a) Stanton, R. E.; Newton, M. D. *J. Phys. Chem.* **1988**, *92*, 2141. (b) Negri, F.; Orlandi, G.; Zerbetto, F. *Chem. Phys. Lett.* **1988**, *144*, 31. (c) Weeks, D. E.; Harter, W. G. *Chem. Phys. Lett.* **1988**, *144*, 66. (d) Brensdal, E.; Cyvin, B. N.; Brunvoll, J.; Cyvin, S. J. *Spectrosc. Lett.* **1988**, *21*, 313. (e) Weeks, D. E.; Harter, W. G. *J. Chem. Phys.* **1989**, *90*, 4744.
(5) Haufler, R. E.; Conceicao, J.; Chibante, L. P. F.; Chai, Y.; Byrne, N. E.; Flanagan, S.; Haley, M. M.; O'Brien, S. C.; Pan, C.; Xiao, Z.; Billups, W. E.; Cuifolini, M. A.; Hauge, R. H.; Margrave, J. L.; Wilson, L. J.; Curl, R. F.; Smalley, R. E. *J. Phys. Chem.* **1990**, *94*, 8634.
(6) Dubois, D.; Kadish, K. M.; Flanagan, S.; Haufler, R. E.; Chibante, L. P. F.; Wilson, L. J. *J. Am. Chem. Soc.* **1991**, *113*, 4364.
(7) Jehoulet, C.; Bard, A. J.; Wudl, F. *J. Am. Chem. Soc.* **1991**, *113*, 5456.
(8) For example: Gosztola, D.; Weaver, M. J. *Langmuir* **1989**, *5*, 776.
(9) Gao, P.; Gosztola, D.; Leung, L.-W. H.; Weaver, M. J. *J. Electroanal. Chem.* **1987**, *233*, 211.
(10) Wilke, T.; Gao, X.; Takoudis, C. G.; Weaver, M. J. *J. Catal.* **1991**, *130*, 62.
(11) For recent descriptions of such real-time potential-dependent SERS tactics, see, for example: (a) Gao, P.; Gosztola, D.; Weaver, M. J. *Anal. Chim. Acta* **1988**, *212*, 210. (b) Gao, P.; Gosztola, D.; Weaver, M. J. *J. Phys. Chem.* **1989**, *93*, 3753.

Figures 1 and 2 show typical potential-dependent sequences of SER spectra obtained for a C_{60} film (two to three monolayers thick) in the 240–840-cm^{-1} and 1080–1620-cm^{-1} frequency regions, respectively, every 10 s during a cyclic voltammogram at 10 mV s^{-1} between 0 and −1.2 V vs $Fc^{+/0}$. (The spectra are limited to 500–600-cm^{-1} segments due to the spatial characteristics of the CCD detector at 647 nm. No significant spectral features were observed from 800 to 1050 cm^{-1}.) The potentials labeled alongside each spectrum are the average values during the data acquistion; the spectra are stacked so that the upward sequence refers to increasing time.

At potentials positive of ca. −0.9 V, the SER spectral features are uniformly quite similar to the normal Raman bands reported for solid bulk-phase C_{60};[1] the frequencies typically match within 5–10 cm^{-1}, and the relative intensities are comparable. A summary of these SER bands, along with the corresponding bulk-phase Raman frequencies, is given in Table I. All 10 Raman active bands anticipated from the bulk-phase selection rules (having A_g or H_g symmetry)[1] are apparently also observed in the SER spectra. Three additional weaker bands are observed, with frequencies that match closely those reported in the bulk-phase infrared spectrum. The one remaining infrared-active band (at 1428 cm^{-1}) is accidentally degenerate with a Raman-active feature. Consequently, then, the SERS selection rules allow the normally exclusively infrared active as well as Raman-active modes of C_{60} to be observed. This symmetry lowering would appear to occur in the absence of C_{60}-surface coordination; the appearance of such Raman-forbidden bands probably reflects the influence of the surface electric-field gradient.[12] The present results differ somewhat from a recent report of SERS for C_{60} on gold in aqueous media, for which a number of additional bands, attributed to distorted C_{60} species, were observed.[2]

The present SERS features are virtually independent of potential between 1.0 and ca. −0.7 V and of the film thickness (from ca. 2 to 20 monolayers). Significant spectral changes, however, occur at potentials between −0.9 and −1.1 V during the forward (negative-going) sweep, which are reversed at ca. −0.6 V during the return sweep (Figures 1 and 2). These potentials correspond precisely to the appearance of the anodic and cathodic waves associated with the formation and reoxidation of C_{60}^- (cf. ref 7).

Several significant elements of these redox-induced spectral changes are evident, as can be seen from Figures 1 and 2 and Table I. First, some of the Raman active bands undergo significant (ca. 5–20 cm^{-1}) frequency downshifts upon formation of C_{60}^- from C_{60}, most prominently for the C_{60} A_g mode at 1460 cm^{-1}, which downshifts by almost 20 cm^{-1}. A comparable frequency downshift for this Raman band has been seen upon doping C_{60} with alkali metals so as to yield conducting films.[13] These effects are indicative of the weakening of C–C bonds caused by the added antibonding electron. Additionally, several bands having H_g symmetry become more intense and broader upon C_{60}^- formation; moreover, two bands (at ca. 710 and 770 cm^{-1}) yield doublets (Figure 1). These changes may well reflect a loss of the usual 5-fold degeneracy of the H_g symmetry bands, arising from anticipated Jahn–Teller distortions in the monoanion.[4b] Sweeping the potential to values negative of −1.4 V, corresponding to C_{60}^{2-} formation, yielded further frequency downshifts of the major Raman features. The bands, however, become markedly weaker and broader. Nonetheless, spectra corresponding to C_{60}^- and C_{60} reappear upon returning the potential to appropriately less negative potentials.

Acknowledgment. Xiaoping Gao provided expert guidance in spectral interpretation. The C_{60} sample was prepared by Joe Roth and Lance Safford. This work is supported by the National Science Foundation and the Office of Naval Research.

(12) (a) Moskovits, M.; DiLella, D. P.; Maynard, K. J. *Langmuir* **1988**, *4*, 67. (b) Moskovits, M. *Rev. Mod. Phys.* **1985**, *57*, 783.

(13) Haddon, R. C.; Hebard, A. F.; Rosseinsky, M. J.; Murphy, D. W.; Duclos, S. J.; Lyons, K. B.; Miller, B.; Rosamilia, J. M.; Fleming, R. M.; Korton, A. R.; Glarum, S. H.; Makhija, A. V.; Muller, A. J.; Erick, R. H.; Zahwak, S. M.; Tycko, R.; Dabbagh, G.; Thiel, F. A. *Nature* **1991**, *350*, 320.

Antibody-Catalyzed Hydrolysis of Phosphate Monoesters

Thomas S. Scanlan, James R. Prudent, and Peter G. Schultz*

Department of Chemistry, University of California Berkeley, California 94720

Received July 18, 1991

Phosphoryl transfer reactions involving tyrosine, serine, or threonine residues play an important biological role in many regulatory and signal transduction processes. Catalysts which selectively phosphorylate or dephosphorylate a given peptide sequence would provide important tools for investigating these systems.[1] One approach to generating catalysts that recognize a specific phosphorylation site takes advantage of the specificity of the antibody molecule.[2] As a first step toward the development of a family of catalytic antibodies for selective phosphoryl transfer reactions, we report the generation of antibodies that catalyze the hydrolysis of an aryl phosphate monoester.

The hapten α-hydroxyphosphonate **1** was synthesized in six steps from α-bromotoluic acid[3] and coupled to keyhole limpet hemocyanin (KLH) via a diazo-linkage reaction to generate an immunogenic conjugate.[4] Balb/C mice were immunized with the

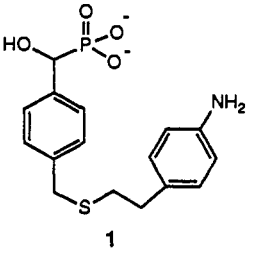

1

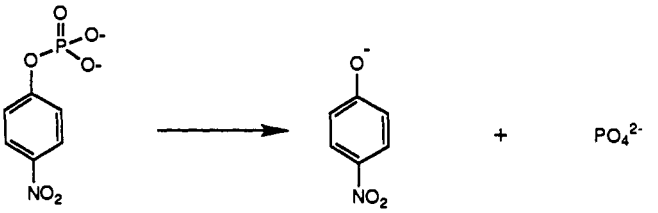

2 (p-NPP)

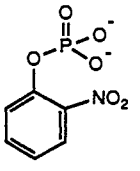

3

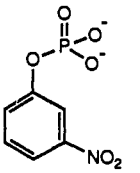

4

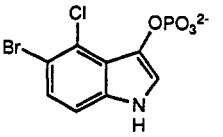

5

protein–hapten conjugate, and 20 hapten-specific hybridoma cell lines were generated using standard hybridoma technology.[5] Monoclonal antibodies from these hybridomas were purified to homogeneity (SDS–polyacrylamide gel electrophoresis) from ascites fluid by protein A affinity chromatography.[6] The antibodies were then assayed spectrophotometrically for their ability

* Author to whom correspondence should be addressed.

(1) For model systems, see: (a) Chin, J.; Banaszczyk, M. *J. Am. Chem. Soc.* **1989**, *111*, 4103. (b) Breslow, R.; Singh, S. *Bioorg. Chem.* **1988**, *16*, 408.

(2) (a) Lerner, R. A.; Benkovic, S. J.; Schultz, P. G. *Science* **1991**, *252*, 659. (b) Schultz, P. G.; Lerner, R. A.; Benkovic, S. J. *Chem. Eng. News* **1990**, *68*, 26.

(3) α-Bromotoluic acid and *p*-nitrophenethyl mercaptan were coupled to form the corresponding thioester–carboxylic acid. Acid chloride formation ($SOCl_2$) followed by an Arbuzof reaction (triethyl phosphite) and carbonyl reduction (DIBAL-H) provided the protected 2-hydroxy aryl phosphonate. Reduction of the nitro group ($SnCl_2$) and phosphonate ester hydrolysis (TMSBr) afforded racemic hapten **1**.

(4) Erlanger, B. *Methods Enzymol.* **1980**, *70*, 85.

(5) Kohler, G.; Milstein, C. *Nature (London)* **1975**, *256*, 495.

(6) Kronvall, G.; Grey, H.; Williams, R. *J. Immunol.* **1972**, *105*, 1116.

0002-7863/91/1513-9397$02.50/0